Essential Readings in Light Metals: Aluminum Reduction Technology.
Edited by Geoff Bearne, Marc Dupuis and Gary Tarcy.

The Surface Chemistry of Secondary Alumina from the Dry Scrubbing Process

A.R. Gillespie*, M.M. Hyland‡, J.B. Metson‡

* Comalco Research and Technical Support
15 Edgars Rd, Thomastown, Victoria 3074, AUSTRALIA

‡ The University of Auckland
Private Bag 92019, Auckland, New Zealand

Abstract

The primary role of dry scrubbing systems at modern aluminium smelters is to prevent discharge of particulate material and, by adsorption on the primary alumina, prevent emission of gaseous hydrogen fluoride to the environment. Dry scrubbers generally return all of the collected material to the electrolytic cell and thus they form an important element in the smelter's mass balance. Return of fluoride is beneficial as it reduces the smelter's requirement to add aluminium fluoride to maintain constant bath ratio. On the other hand return of hydrogen, in the form of adsorbed water, HF, or chemically bound hydroxyl groups, is not beneficial as it provides a pathway for re-generation of HF in the electrolyte.

The products of the dry scrubbing reaction are not well described in the literature. In particular, it has not been possible to determine the form and relative distribution of hydrogen in the dry scrubber product. This paper presents the results of spectroscopic investigations of hydrofluorinated alumina that show water and fluoride to be bound in the form of a hydrated aluminium-hydroxyfluoride phase of variable stoichiometry. Hydrogen therefore occurs as water of hydration that is easily removed at relatively low temperatures, and as hydroxyl groups that are stable to higher temperatures. Hydrogen fluoride release may occur as a result of self hydrolysis of the hydroxyfluoride, or by reaction with the molten electrolyte.

Introduction

The dry scrubbing process at aluminium smelters captures gaseous hydrogen fluoride and particulate solids, thereby minimising emission of these materials to the environment. In addition to fluoride, the product stream from a dry scrubber contains impurity elements that are also returned to the electrolysis cell. Amongst the impurities is hydrogen, possibly in the form of adsorbed molecular water or hydrogen fluoride, or chemically bound hydroxyl groups

Since the advent of dry scrubbing in the 1960's, the process has been described in patents and various scientific and industrial publications. The former consider engineering aspects related to improving gas/solid contacting and solids collection efficiency, while the latter also consider the chemical mechanism of HF adsorption. Both types of information may be used to develop process models describing leverage points for improving HF capture efficiency and the control and utilisation of fluoride in the smelter.

Among the first to investigate the adsorption mechanism were Cochran [1] and Cochran *et al* [2], who measured HF adsorption capacities after hydro-fluorinating smelter grade alumina in a pilot scale dry scrubber. Their major conclusion was that HF adsorption is reversible at 120°C, implying that the maximum quantity of HF that can be adsorbed under a particular set of conditions is proportional to the partial pressure of HF in the gas phase. This finding was generally accepted. For example, on the basis of a limited data set, Lamb [3] demonstrated good agreement with the Langmuir model of reversible monolayer formation.

Recently published data [4] suggests that HF adsorption is, in fact, irreversible at typical dry scrubbing temperature and should be considered in terms of a rectangular isotherm. In terms of the HF concentration achievable at the dry-scrubber outlet, the rectangular isotherm implies that there is no lower limit. Provided that gas/solid contact can be maintained on the time scale dictated by chemical reaction or mass transfer processes, it should be possible to reduce the HF concentration in the reactor outlet to near zero levels, whilst maintaining high levels of adsorbed fluoride on the alumina. Furthermore, irreversible adsorption implies a level of stability such that fugitive emission may be unlikely during transfer of the reacted alumina to the electrolysis cell.

Although the literature provides useful data regarding the fluoride adsorption capacities of various alumina samples (see the review of Hyland *et al* [5]), there is little agreement as to the mode in which fluoride and hydrogen are bound to the alumina surface. Lack of consensus appears to result mainly from the researchers' need to infer the structure of the products of reaction from adsorption capacity and adsorbent surface area data, and from previously published investigations of adsorbent and adsorbate structure.

For example, it was postulated by Cochran [1,2] that a chemisorbed monolayer of $F(O)_3$ tetrahedrons forms at the alumina surface (Figure 1a). In that model, the surface was considered as a truncation of the bulk alumina structure, with adsorption occurring at the 1/3 of the spaces between surface oxygen ions that are unoccupied by interstitial Al^{3+} ions.

Lamb [3] postulated that any of the various surface hydroxyl groups on alumina can be substituted by fluoride, thereby ejecting a water molecule (Figure 1b). Adsorption to form multilayers was postulated to occur by hydrogen bonding between fluoride ions already adsorbed, and further HF molecules (Figure 1c). Lamb suggested that in the presence of water vapour the multilayers are stabilised by adsorbed water (Figure 1d), and that the strength of the hydrogen bonds diminishes as they became more remote from the original surface.

In contrast to Lamb's model which predicted a direct Al-F interaction in the first layer, Bavarez and De Marco [6] proposed that molecular HF forms hydrogen bonds with localised water molecules on the alumina surface (Figure 1e). Additional water

was thought to stabilise the initial HF layers and to provide a surface for adsorption of further bimolecular HF layers (Figure 1f). Adsorption was considered to virtually cease after the formation of the "quadruple layer", due to the diminishing attractive effect of the adsorbent surface.

Coyne *et al* [7,8] considered the Bavarez and De Marco model inadequate to describe HF adsorption from a dry gas stream. It was assumed that because a significant quantity of HF could be adsorbed under dry conditions, it was unlikely that the initial layer in the adsorption process would be molecular water. Instead, Bavarez and De Marco proposed that HF formed hydrogen bonds directly with surface hydroxyl groups and in the presence of water vapour a multilayer structure would be built up (Figure 1g).

From the spectroscopic data presented in the open literature, there is little direct support for the models referred to above. Cochran anticipated the formation of AlF_3 in hydro-fluorinated alumina but could not detect the crystalline phase by powder X-ray diffraction (XRD). However AlF_3 did form when the material was heated above 300°C. Lobos *et al* [9] and Burkat *et al* [10] reported similar findings. Using solid state ^{19}F and ^{27}Al NMR the latter showed that some of the adsorbed fluoride forms coordinative bonds with the alumina surface, yet is still relatively mobile, while other fluoride forms bridges between aluminium ions and is of low mobility.

Using X-ray photoelectron spectroscopy (XPS), Lamb was able to identify a NaF interaction in hydro-fluorinated alumina, but could not discern an Al-F interaction. Haverkamp *et al* [11] and Hyland *et al* [12] also observed an Na-F interaction, however for samples obtained from a dry scrubber it was not possible to distinguish between NaF and particulate sodium fluoro-aluminate. In laboratory prepared samples that had been hydro-fluorinated in moist gas, XPS spectra showed no bonding interaction between Al and F ions, although the dry scrubber sample demonstrated a slight asymmetry to high binding energy, possibly indicative of Al-F bonding. This was thought to be due to fluoride particulate such as $NaAlF_4$ and Na_3AlF_6. When alumina was predried for 12 hours at 300°C and hydro-fluorinated in dry gas, the surface concentration of fluoride increased by a factor of 4.5 and the spectra were consistent with the formation of β-$AlF_3.3H_2O$.

At best the models that appear in the literature are supported by circumstantial evidence. There was, therefore, sufficient justification for further investigation of the adsorption mechanism, and in particular the surface structure of the hydro-fluorinated SGA. The following sections describe spectroscopic and thermo-gravimetric studies of laboratory prepared samples.

Experimental

The objective of laboratory scale experiments was to adsorb HF under conditions similar to those encountered in typical dry scrubbers. Due to the difficulties of handling and mixing anhydrous HF with other gases, the experimental apparatus was designed around vapourisation of aqueous HF solutions. A laboratory scale rig, similar those used by others [3,6,7,8], was constructed and has been described elsewhere [4]. For the hydro-fluorinated SGA samples described in the following sections, adsorption took place under the following conditions: $[HF]_{inlet}$ = 60 mg Sm^{-3}, T = 80°C, relative humidity = 3.8 %.

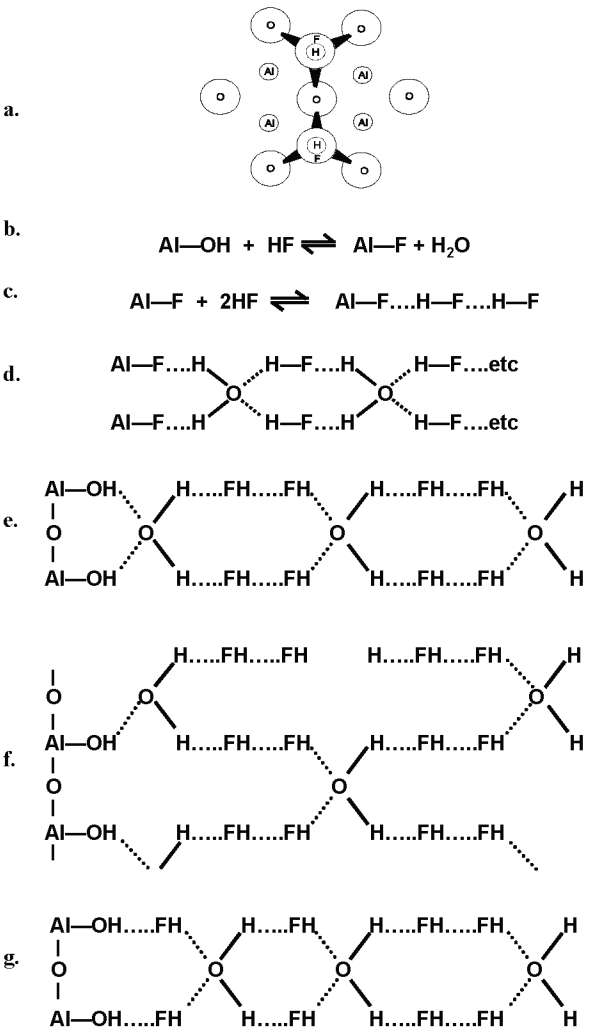

Figure 1: Models of the hydro-fluorinated alumina surface by; (a) Cochran, (b,c,d) Lamb, (e,f) Bavarez and De Marco, and (g) Coyne *et al*.

XRD patterns were measured with a copper source operating at 40 kV and 20 mA. The goniometer was a Phillips PW1050/25 with graphite monochromator, controlled by Sietronics automated software via a Sietronics Sie-Ray 112 controller. Angle calibration was carried out against the 111 reflection of metallic silicon (two-theta = 28.422° for Cu $K\alpha_1$). Samples were floated onto a flat microscope slide in an isopropanol slurry, or pressed into a dished microscope slide.

XPS spectra were measured on a Kratos XSAM 800 utilising non mono-chromatised aluminium or magnesium X-rays from a dual anode gun operating at 216 W electrical power. The kinetic energy analyser was of the hemispherical type operating in fixed analyser transmission (FAT) mode. Low and high-resolution scans were obtained at pass energies of 65 eV and 20 eV respectively. Typically, analytical chamber pressure was in the range 5 - 50 x 10^{-10} Torr. Peak deconvolution was by a linear least squares method using mixed Gaussian/Lorentzian functions.

Magic angle spinning, solid state NMR (MAS-NMR) spectra of ^{27}Al, ^{19}F and ^{23}Na, were recorded in a Bruker MSL 400 spectrometer with a nominal field of 9.4 Tesla. Samples were contained in 4 mm PSZ rotors at a rotation speed of 12 kHz.

DSC traces were measured with a Polymer Laboratories heat-flux DSC. Heat flow was determined by calibrating the instrument with 99.999% indium, while calibration of the baseline for changes in heat capacity over a broad temperature range was achieved with α-alumina. Typical sample size was 10 mg and all experiments were conducted under dry nitrogen, using matched sample and reference crucibles. Larger scale heating experiments were conducted in a nitrogen flushed, transparent gold furnace, with off gas analysis by IR spectroscopy

Characterisation of Hydro-Fluorinated SGA

Under typical dry-scrubber gas composition and temperature conditions, adsorption of HF had little effect on the morphology and phase composition of SGA (Figures 2a and 3a), despite adsorption of 7.0 wt% fluoride. This suggests that the adsorbed fluoride was highly dispersed, and is consistent with the high specific surface area (73 m^2/g here) that results from the presence of transition alumina phases in SGA.

Long-term ageing of the hydro-fluorinated SGA under dry conditions did not affect the morphology or phase composition of the particles (Figures 2b and 3b). However high humidity ageing at room temperature, subsequent to hydro-fluorination, resulted in rapid and dramatic changes in particle morphology and phase composition. SEM images (Figure 3c) demonstrate the appearance of numerous small crystallites on the wet-aged particle's outer surfaces, while XRD indicated the presence of the crystalline phase $AlF_x(OH)_{3-x}.nH_2O$, aluminium hydroxy-fluoride (Figure 2c).

Following the appearance of $AlF_x(OH)_{3-x}.nH_2O$ after high humidity ageing, it was postulated that unaged samples might also contain the hydroxy-fluoride phase, although in a form not detectable by SEM or XRD. The absence of distinct morphological and phase composition changes as a result of hydro-fluorination, would not be unexpected if the resulting phase were highly dispersed on the SGA surface, and thus had crystalline domains too small for coherent X-ray diffraction. The remainder of this section describes experiments that were aimed at distinguishing such an *amorphous* $AlF_x(OH)_{3-x}.nH_2O$ layer, from stratified layers such as postulated by Cochran, Lamb, Bavarez and DeMarco and Coyne *et al.*

In the remainder of this paper, smelter grade alumina will be referred to as SGA, hydro-fluorinated smelter grade alumina will be referred to as *amorphous*. High humidity aged, hydro-fluorinated smelter grade alumina will be referred to as *crystalline*.

Amorphous & *Crystalline* Hydro-fluorinated SGA.

As anticipated, amorphous and crystalline samples contained significant surface fluoride (Table 1), as determined from XPS survey scans. The surface fluoride levels bracketed literature values for samples obtained under similar hydro-fluorination conditions [11]. The considerable scatter in surface elemental composition of various samples, suggests that the resulting

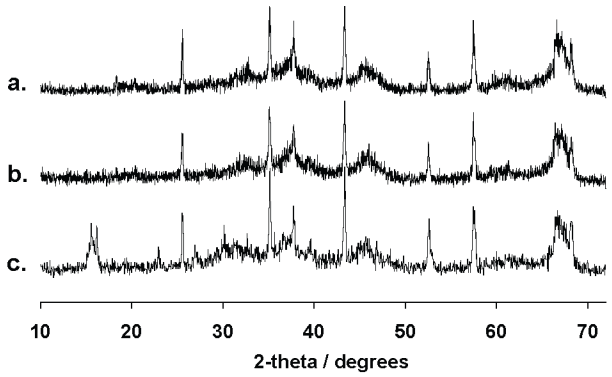

Figure 2: Powder XRD patterns of; (a) SGA, (b) *amorphous* and (c) *crystalline,* hydro-fluorinated SGA.

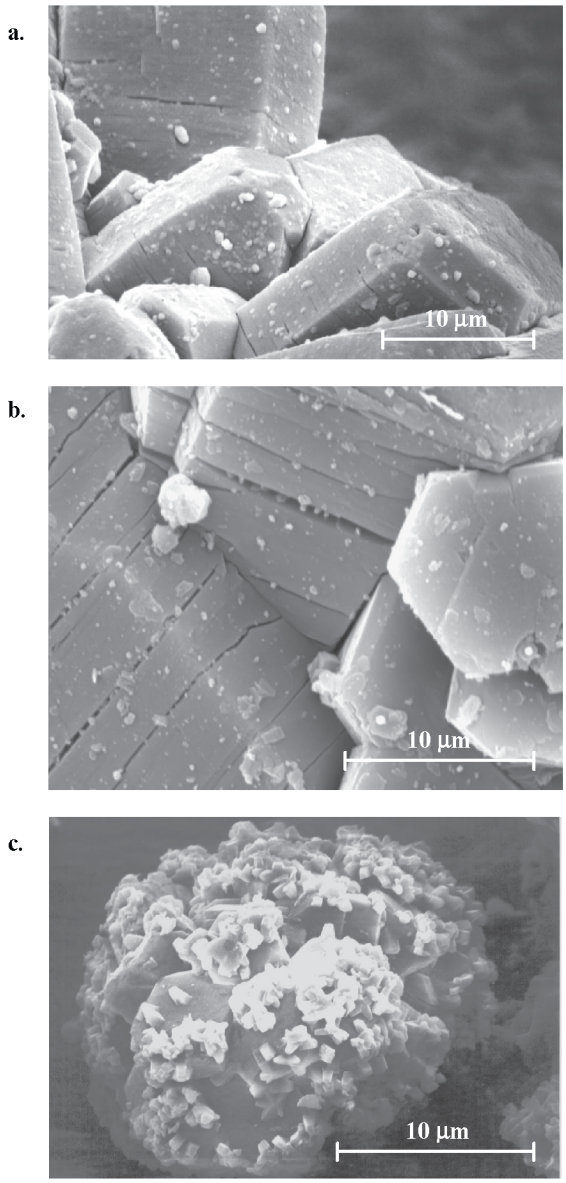

Figure 3: SEM images of; (a) SGA, (b) *amorphous* and (c) *crystalline,* hydro-fluorinated SGA.

surfaces are unstable, and not fully equilibrated prior to surface analysis. In this case the major factor affecting the surface elemental composition may have been the time between hydro-fluorination and surface analysis, which ranged between days and weeks.

For the amorphous samples, high resolution XPS spectra showed slight asymmetry on the high BE side of the Al2p peak (Figure 4). The Al2p peaks of the crystalline sample were symmetric, but broader and of higher BE than those of SGA. For both amorphous and crystalline samples the Al2p peaks were fitted with an additional component having a binding energy of 75.5 eV, intermediate between that of SGA and the tri-fluorides AlF_3 and $AlF_3.3H_2O$. By allowing for some variability in the measured position of the Al2p peak, spectra reported by Haverkamp *et al* [11] for un-aged hydro-fluorinated SGA (*ie* amorphous) are indistinguishable from those presented here. Although apparent in their spectra, Haverkamp *et al* did not attempt to fit a high BE component to the Al2p peak envelope.

The appearance of a component at intermediate binding energy suggests that, compared with the tri-fluorides, fluoride only partially replaces hydroxide or oxide, thus perturbing the aluminium ion to a lesser extent than occurs in the tri-fluorides. This is consistent with the formation of $AlF_x(OH)_{3-x}.nH_2O$ although it may also support Lamb's model of Al-F Lewis bonds at the alumina surface.

Böse *et al* [13] report XPS spectra of various crystalline phases including transition alumina, AlF_3 and $AlF_{2.3}(OH)_{0.7}.H_2O$. The spectra were static charge referenced using distributed 20 nm gold particles (rather than the more commonly used 1s peak of adventitious carbon), thus making direct comparison of binding energies with this work inaccurate. However the published Al2p binding energy shifts relative to alumina, can be compared directly with the BE shifts obtained here. Table 2 demonstrates good agreement with the published BE shifts, provided that the SGA surface is considered to be α-Al_2O_3. This assumption is not unreasonable and is supported by the data of Roach *et al* [14] who published Environmental-SEM micrographs showing that, as a result of rapid calcination, α-Al_2O_3 forms at the surfaces and edges of SGA.

Solid state MAS-NMR spectroscopy provides further support for the partial substitution of fluoride for hydroxide. The ^{27}Al spectrum of SGA has the appearance (Figure 5d) of a spectrum of a typical transitional alumina phase with 1:3 ratio of tetrahedral (AlO_4) to octahedral (AlO_6) sites (see Smith [15]). The ^{27}Al spectra of amorphous and crystalline samples (Figure 5b,c), demonstrate perceptible additional structure at negative shift values. This is consistent with the formation of either tri-fluoride (Figure 5a) or hydroxy-fluoride.

As a result of hydro-fluorination, octahedral aluminium content decreased from 24.5% to 19.4%, thus indicating that 4.9% of aluminium ions had become associated with fluoride in either a trifluoride or hydroxy-fluoride form. It is unlikely that monolayer substitutution as proposed by Lamb, would result in such a change in symmetry. Further, using statistical [16] or experimental [17] techniques, the number of aluminium ions at transition alumina surfaces has been shown to be on the order of 2-3 per square nanometre. For SGA having specific surface area of 74 $m^2 g^{-1}$, this equates to only 1.2 – 2.5 % of the total number of aluminium ions, therefore Lamb's model, which assumes a monolayer of Al-F bonds, is unlikely to be valid.

Table 1: Surface elemental composition.

Adsorbent	Al	O	F	C	Na
This investigation					
SGA	1	1.8	<0.1	0.4	0.04
Amorphous	1	1.8	0.3	2.1	-
Crystalline	1	1.9	0.3	0.8	-
Literature					
Haverkamp *et al* [11]	1	1.2	0.3	-	0.1
Hyland *et al* [12]	1	-	0.7	-	0.06

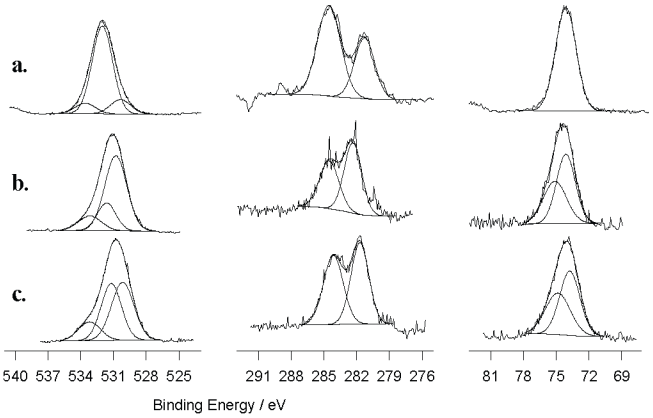

Figure 4: XPS spectra of; (a) SGA, (b) amorphous hydro-fluorinated SGA, and (c) hydro-fluorinated SGA aged at high humidity.

Table 2. Surface Chemical Composition.

Adsorbent	Al2p Binding Energy / eV 5/2	3/2	Average	ΔBE / eV
This investigation.				
SGA	-	-	74.1	0
Amorphous	-	-	74.1	0
			75.5	1.4
Crystalline	-	-	74.1	0
			75.6	1.4
Böse et al [13].				
α-Al_2O_3	74.68	74.55	74.62	-
γ-Al_2O_3	74.21	74.05	74.13	-
α-$Al(OH)_3$	74.12	73.97	74.05	-
γ-$Al(OH)_3$	74.11	73.96	74.04	-
γ-AlO(OH)	74.17	74.03	74.10	-
$AlF_{2.3}(OH)_{0.7}.H_2O$	76.04	75.90	75.97	1.35*
α-AlF_3	77.27	77.15	77.21	2.59*
β-AlF_3	77.51	77.37	77.44	2.82*

* Relative to α-Al_2O_3

The ^{19}F NMR spectra of the amorphous and crystalline samples are similar (Figure 6b,c), indicating the structural similarity of the two fluoride bearing phases. The spectra differ markedly from the ^{19}F spectrum of AlF_3 (Figure 6a), which is characterised by a downfield shift of –6.8 ppm. Sodium was present in all of the samples, as evidenced by the XPS and ^{23}Na MAS-NMR spectra (Figure 7). Magic angle spinning had little effect on the appearance of the sodium spectrum, suggesting that sodium occupies a disordered environment.

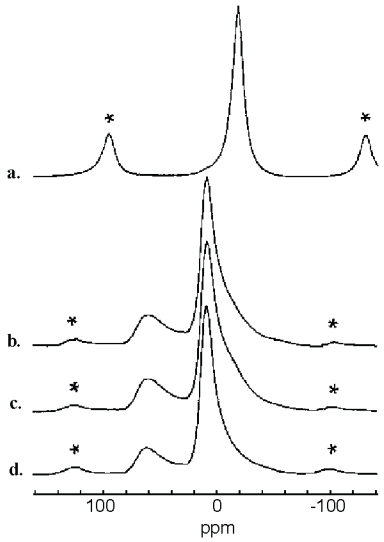

Figure 5. ^{27}Al MAS-NMR spectra of; (a) AlF_3, (b) amorphous hydro-fluorinated SGA, (c) crystalline hydro-fluorinated SGA, (d) SGA. Chemical shift values in ppm relative to aqueous $AlCl_3$. Peaks labelled * represent spinning spinning sidebands.

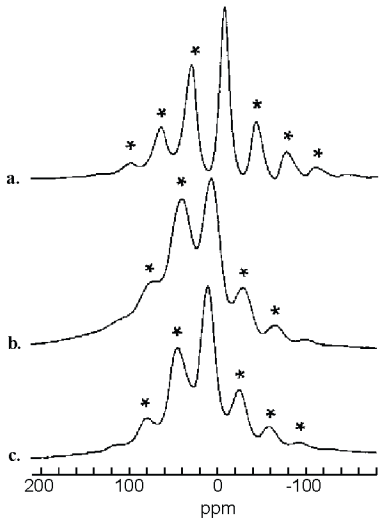

Figure 6. ^{19}F MAS-NMR spectra of; (a) AlF3, (b) crystalline hydro-fluorinated SGA, (c) amorphous hydro-fluorinated SGA. Chemical shift values in ppm relative to C_6F_6. Peaks labelled * represent spinning spinning sidebands.

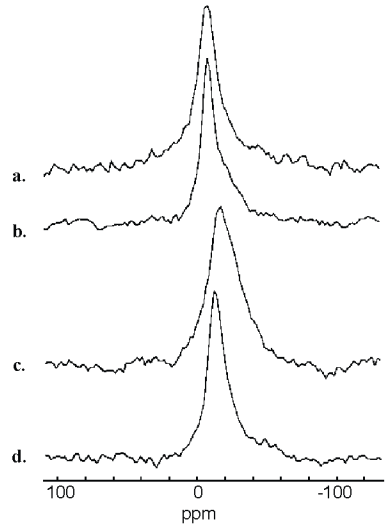

Figure 7. ^{23}Na MAS-NMR spectra of; (a,b) SGA, (c) amorphous hydro-fluorinated SGA, (d) crystalline hydro-fluorinated SGA. Chemical shift values in ppm relative to aqueous NaCl.

For amorphous hydro-fluorinated SGA, water loss was observed to occur in the temperature range 100 – 400°C, whereas fluoride loss (as HF) was observed to start above 440°C (Figure 8). Dehydration of the underlying alumina is observed to start at approximately 540°C for both SGA and amorphous hydro-fluorinated SGA. This supports the formation of the hydroxy-fluoride phase, for which Cowley and Scott [18] have demonstrated the relative lability of the water molecule in the crystal lattice. Separate loss of water and fluoride from stratified layers of HF and H_2O - as in the models of Lamb, Bavarez and Demarco, Coyne and Cochran - is difficult to reconcile with the data. For these models it would be anticipated that water and HF would be released together.

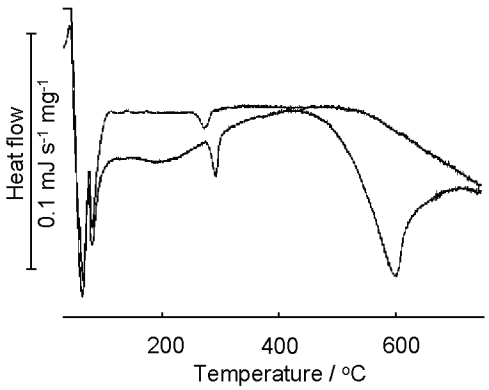

Figure 8. Differential Scanning Calorimeter trace of smelter grade alumina. Heating rate 1°C min^{-1}. Exotherms ↑, endotherms ↓.

During intermediate storage of hydro-fluorinated SGA, and transport between dry scrubber and pot-room, the dry scrubber product would be expected to remain relatively stable and with little or no water or fluoride loss, provided that the temperature does not exceed 100°C. However, during storage in cell hoppers and particularly during cell feeding - where the alumina experiences a dramatic and sudden increase in temperature – the secondary alumina may decompose to release HF. The following reactions are postulated as likely decomposition pathways:

$$AlF_2(OH)_{(s)} \rightarrow AlFO_{(s)} + HF_{(g)} \quad (1)$$

$$AlF(OH)_{2(s)} \rightarrow AlOOH_{(s)} + HF_{(g)} \quad (2)$$

$$2AlOOH(s) \rightarrow Al_2O_{3(s)} + H_2O_{(g)} \quad (3)$$

The solid product of reaction 1 has stoichiometry equivalent to species that are postulated to occur in the electrolyte [19]. The solid product of Reaction 2 has stoichiometry equivalent to Bohemite or Diaspore - the known oxy-hydroxide phases of aluminium - and may therefore decompose (Reaction 3) to form similar products. The literature [20] suggests decomposition of Boehmite starts at above 300°C. It is likely that by the time the particles reach the onset temperature for self-hydrolysis and oxy-hydroxide decomposition, the hydro-fluorinated SGA would have become fully submerged in the electrolyte. Therefore it may reasonably be assumed that hydrogen carried by hydro-fluorinated SGA may also react directly with the electrolyte itself.

Conclusions

Previous models of the surfaces of hydro-fluorinated SGA are inconsistent with the data presented in this paper. In particular, it is difficult to reconcile models that postulate stratified layers of HF and water, with the observed water loss, then HF loss, that occurs as the material is heated.

Instead, the spectroscopic and thermo-gravimetric data appear consistent with the formation of a layer of aluminium hydroxy-fluoride. Due to the highly distributed form of the layer, morphological changes cannot be discerned, and the layer appears amorphous to XRD. The specific elemental composition of the hydroxy-fluoride layer has not been unequivocally established, may be variable, and may depend on the aging history of the sample.

In the absence of a direct measurement of hydrogen ion content, it is difficult to predict the exact level of hydrogen in the dry scrubber product. Nevertheless the behavior of the dry scrubber product stream can be postulated, at least in terms of fluoride and water loss during transport between the dry scrubber and cell hopper, and during cell feeding.

In the former, it is likely that loss of water from the hydroxy-fluoride lattice occurs, resulting in the phase $AlF_x(OH)_{3-x}$. In the latter, self hydrolysis may occur above or within the electrolyte, as the particles are heated during cell feeding. Alternatively the dehydrated product may react directly with the electrolyte to form HF. There may, therefore, be multiple routes to HF formation.

Acknowledgement:

Financial support from Comalco Research Centre is gratefully acknowledged. Assistance in measuring and interpreting NMR spectra was provided by Dr T. Bastow, CSIRO – Division of Materials Science and Technology.

References

[1] C.N. Cochran, *Env. Sci. Technol.,* **8 (1) ,** 63, (1974)

[2] C.N. Cochran, W.C. Sleppy, W.B. Frank, *Journal of Metals,* **22 (9)**, 54, (1970).

[3] W.D.Lamb, *Light Metals 1978,* Ed. J.J. Miller, 425 (1978)

[4] A.R. Gillespie, M.M. Hyland, J.B. Metson, *Journal of Metals,* **51 (5)**, 30-32, (1999).

[5] M.M. Hyland, J.B. Metson, R.G Haverkamp, *Proceedings of 4th Australasian Aluminium Smelting Technology Workshop*, Sydney, Australia, 117, (25 - 30 October 1992).

[6] M. Bavarez, R. De Marco, *Journal of Metals,* **32**, 10, (1980).

[7] J.F. Coyne, M.S. Wainwright, M.P. Brungs, A.N. Bagshaw, *Light Metals 1987,* Ed. R.D. Zabreznik, 35, (1987).

[8] J.F. Coyne, P.J. Wong, M.S. Wainwright M.P. Brungs, *Light Metals 1989*, Ed. P.G. Campbell 113, (1989).

[9] J.S.Lobos, J.P. McGeer D.P Sanderson, *Light Metals 1971,* Ed. T.G. Edgeworth, 455, (1971).

[10] V.S. Burkat, V.S. Dudrova, V.S. Smola, T.S. Chagina, *Light Metals 1985,* Ed. H.O. Bohner, 1443, (1985).

[11] R.G. Haverkamp, J.B. Metson, M.M. Hyland, B.J. Welch, *Surf. Interface Anal.,* **19,** 139, (1992).

[12] M.M. Hyland, J.B. Metson, R.G. Haverkamp, B.J. Welch, *Light Metals 1992,* Ed. E.R. Cutshall, 1323, (1992).

[13] O. Böse, E. Kemnitz, A. Lippitz, W.E.S. Unger, *Fresenius J. Anal. Chem*., **358**, 175-179, (1997).

[14] G.I.D. Roach, J. Cornell, J. Dunn, C. Kleppe, *Proceedings of 3rd International Alumina Quality Workshop,Hunter Valley, Australia,* 200, (1993).

[15] M.E. Smith, *Appl. Magn. Reson.,* **4,** 1 (1993).

[16] R. Zhou and R.L. Snyder, *Acta Crystallographica,* **B47(5)**, 617, (1991)

[17] E.B. Cornelius, T.H. Milliken, G.A. Mills, A.G. Oblad, *J. Phys. Chem.,* **59**, 10, 809, (1955)

[18] J.M.Cowley, T.R.Scott, *J. Am. Chem. Soc.,* **70**, 105, (1948).

[19] K. Grjotheim and B.J. Welch, *Aluminium Smelter Technology,* Aluminium Verlag (1988)

[20] K. Wefers, C. Misra, *Oxides and Hydroxides of Aluminium*. Alcoa Technical Paper No. 19, Alcoa Laboratories (1987).